Sivers distribution functions of sea quarks in a proton with the chiral Lagrangian

Fangcheng He[1,2] and P. Wang[1,3]
[1]Institute of High Energy Physics, CAS, P.O. Box 918(4), Beijing 100049, China
[2]School of Physics, University of Chinese Academy of Sciences, Beijing 100049, China
[3]Theoretical Physics Center for Science Facilities, CAS, Beijing 100049, China

(Received 16 April 2019; published 29 October 2019)

We propose a mechanism for the Sivers distribution function in a proton with the chiral Lagrangian. By introducing the gauge link of the vector meson, the transverse momentum dependent distribution of a pion in the nucleon is redefined, which is locally $SU(2)_V$ invariant as the Lagrangian. The eikonal propagator is generated from the gauge link, and this scenario is proven to be equivalent to the final state interaction. By combining the calculated splitting function and the valence $\bar{q}$ distribution in π from the recent fit, the sea quark Sivers function in a proton is obtained. We find reasonable numerical results for the first momentum $x\Delta^N f_{\bar{q}}^{(1)}(x)$ without any fine tuning of the free parameters.

DOI: 10.1103/PhysRevD.100.074032

I. INTRODUCTION

In the recent decades, the transverse partonic structure of hadrons has been the subject of a lot of theoretical and experimental investigations. The so called transverse momentum dependent (TMD) parton distributions are of great interest since they offer insight in the three-dimensional structure of hadrons in terms of the QCD degrees of freedom (d.o.f.) [1]. At leading twist there are totally eight TMD parton distributions. Among them, two distributions, i.e., Boer-Mulders (BM) and Sivers distributions, are time-reversal odd [2]. Compared with the BM distributions, more data of Sivers distributions were extracted from semi-inclusive deep inelastic scattering (SIDIS) collected by the HERMES and COMPASS collaborations [3,4]. Sivers function describes the asymmetric distribution of unpolarized quarks in a transversely polarized parent hadron. It is very essential to explain the single-spin asymmetries (SSAs) in SIDIS which have been observed experimentally for a long time [5–7].

Theoretically, it is very difficult to calculate parton distribution functions (PDFs) from the first principle due to the nonperturbative behavior of QCD. Since PDFs are defined in Minkowski space, originally, it is also impossible to simulate on the Euclidean lattice. Though the quasi-PDFs are proposed to be calculated on lattice based on the large momentum effective theory (LaMET) [8], the simulation of PDFs on lattice is still in the early stage. For the Sivers distribution function, most calculations are based on the phenomenological quark models, such as the spectator model [9–16], the MIT bag model [17], the constituent quark model [18,19], etc. In these model calculations, the gluon field is introduced as the gauge link. The T-odd parton distributions are zero without this gauge link because of the time reversal invariance. Dynamically, T-odd PDFs emerge from the gauge link structure of the parton correlation functions which describe the initial/final state interactions [20,21].

In the deep inelastic scattering (DIS) process, the calculations of meson cloud effects were performed by Sullivan, where the nucleon is composed of mesons (pions, kaons) and a bare baryon [22]. It is well known that effective field theory (EFT) is a very good and systematic method to study hadron physics. There are a lot of applications of EFT on the hadron spectrum, form factors, and hadron-hadron interaction. In particular, for the parton distributions, it can be obtained from the convolution form, where the splitting function can be derived with the chiral Lagrangian [23,24]. Without fine tuning, the obtained PDFs as well as the integrated moments are in reasonable agreement with the experimental data [25,26]. However, there is no such kind of calculation for the T-odd TMD PDFs with EFT. The reason is that on the one hand, if we use the same approach, the splitting function is zero for the Sivers distributions. One the other hand, the colored gluon field introduced from the gauge link is not consistent with the framework of EFT which is formulated in terms of hadronic d.o.f.

Therefore, in this paper, we will provide a mechanism to generate the T-odd TMD PDFs with the chiral Lagrangian.

The bilocal operator constructed for the splitting function is invariant under the flavor $SU(2)$ symmetry instead of color gauge symmetry. With this approach, we will calculate the sea quark Sivers distribution functions in a proton, which have not been estimated theoretically even in the quark models. Sea quark Sivers functions are important to explaining azimuthal asymmetries for $\pi^{\pm}$ and $K^{\pm}$ production off a proton target in SIDIS and the asymmetrical cross sections for a vector boson in the polarized Drell-Yan process [27,28]. It is also crucial to testing the sign change of Sivers functions between SIDIS and the Drell-Yan process. Though the sea quark Sivers functions have been extracted from the experiments [29–32], the theoretical explanation is still lacking. The calculation here is for the Sivers functions of sea quarks in a proton, and it is straightforward to generally apply it to any T-odd distributions.

II. SIVERS DISTRIBUTION FUNCTION

For the quark flavor q, according to the Trento convention, the unpolarized and Sivers distributions $f_1(x,\vec{k}_\perp)$ and $f_{1T}(x,\vec{k}_\perp)$ are defined as [33]:

$$f_1^q(x,\vec{k}_\perp)+\frac{\epsilon^{ji}k_\perp^i S_\perp^j}{m_p}f_{1T}^q(x,\vec{k}_\perp) =\frac{1}{2}\int\frac{d\xi^- d^2\vec{\xi}_\perp}{(2\pi)^3}e^{-ixP^+\xi^-+i\vec{k}_\perp\cdot\vec{\xi}_\perp}\langle P,\vec{S}_\perp|\mathcal{O}^q|P,\vec{S}_\perp\rangle, \quad (1)$$

where $\vec{S}_\perp$ is the transverse spin of a proton. The gauge invariant bilocal operator $\mathcal{O}^q$ is defined as [34]:

$$\mathcal{O}^q=\bar{q}(\xi^-,\vec{\xi}_\perp)\mathcal{L}^\dagger_{\xi_\perp}(\infty,\xi^-)\gamma^+\mathcal{L}_0(\infty,0)q(0,0), \quad (2)$$

where $\mathcal{L}$ is the path-ordered light-cone color gauge link expressed as

$$\mathcal{L}^\dagger_{\xi_\perp}(\infty,\xi^-)=Pe^{-ig_c\int_{\xi^-}^{\infty}A^+(z^-,\vec{\xi}_\perp)dz^-}. \quad (3)$$

Similar to the quark distribution, for the pion distribution, i.e., the splitting function, the operator can be defined from the light-cone bilocal meson operator as

$$\mathcal{O}^{\pi^+}=i[\pi^-(y^-,\vec{y}_\perp)\partial^+\pi^+(0)-\partial^+\pi^-(y^-,\vec{y}_\perp)\pi^+(0)]. \quad (4)$$

This kind of operator based on hadronic d.o.f. has been applied for the calculation of pion distributions in the EFT [25,35]. However, the above operator gives no contribution to the T-odd Sivers function. Therefore, we need to construct a bilocal operator for the meson fields which has the time reversal asymmetry. In Refs. [36–38], vector meson V_μ is introduced as a dynamical gauge boson to guarantee the local $SU(2)_V$ hidden symmetry. The matrix of V_μ is written as

$$V^\mu=\vec{\rho}^{\,\mu}\cdot\vec{\tau}=\begin{pmatrix}\frac{1}{\sqrt{2}}\rho^0 & \rho^+\\ \rho^- & -\frac{1}{\sqrt{2}}\rho^0\end{pmatrix}^\mu. \quad (5)$$

The Lagrangian for the meson fields can be written as

$$\mathcal{L}=f_\pi^2\mathrm{Tr}[\alpha_\mu\alpha^\mu], \quad (6)$$

where α_μ is defined as

$$\alpha_\mu=\frac{1}{2i}(D_\mu\xi_L\cdot\xi_L^\dagger-D_\mu\xi_R\cdot\xi_R^\dagger). \quad (7)$$

The covariant derivatives are expressed as

$$D_\mu\xi_{L/R}=\partial_\mu\xi_{L/R}+igV_\mu\xi_{L/R}+i\xi_{L/R}L_\mu/R_\mu, \quad (8)$$

where L_μ and R_μ are the external fields. The coupling constant $g=g_{\rho\pi\pi}/\sqrt{2}$ and $g_{\rho\pi\pi}$ is related to the vector meson mass M_ρ through the Kawarabayashi-Suzuki-Fayyazuddin-Riazuddin relation $M_\rho^2=2g_{\rho\pi\pi}^2f_\pi^2$ [39,40]. $f_\pi=92.1$ MeV is the pion decay constant [41]. In the chiral Lagrangian, $\xi_L^\dagger=\xi_R=\xi=\exp(i\pi/f_\pi)$ with $\pi=\vec{\pi}\cdot\vec{\tau}/\sqrt{2}$. When matching quark currents to the hadron level, L_μ and R_μ are expressed as $L_\mu=R_\mu=\tau_q v_\mu$, where $\tau_q=\mathrm{diag}(\delta_{qu},\delta_{qd})$ are diagonal 2×2 quark flavor matrices. v_μ is the external vector field. From Eq. (6), we can get the local current for a given quark flavor [24]. To get the bilocal operator at the hadron level, the nonlocal action is written as

$$\mathcal{S}=\int dx\,dy\,f_\pi^2\mathrm{Tr}[\alpha_\mu(y)W(y,x)\alpha^\mu(x)W^\dagger(y,x)], \quad (9)$$

where the gauge link function $W(y,x)$ is introduced to guarantee the nonlocal Lagrangian is locally $SU(2)_V$ invariant like the local one. $W(y,x)$ is defined as

$$W(y,x)=Pe^{I(x,y)}=Pe^{-ig\int_x^y dz_\nu V^\nu(z)}. \quad (10)$$

At the leading order of g, the current that couples to the external field v_μ can be obtained from Eq. (9) as

$$\mathcal{J}^\mu_{q/\pi}=2i\mathrm{Tr}\{[\partial^\mu\pi(y)\pi(x)-\pi(y)\partial^\mu\pi(x)]\tau_q +\partial^\mu\pi(y)[I(x,y),\pi(x)\tau_q]+\partial^\mu\pi(x)[I(x,y),\tau_q\pi(y)]\}. \quad (11)$$

For example, the current for the $\bar{d}$ quark in π^+ is written as

$$\mathcal{J}^\mu_{\bar{d}/\pi^+}=i[\pi^-(y)\partial^\mu\pi^+(x)-\partial^\mu\pi^-(y)\pi^+(x)] \times\left[1-i\sqrt{2}g\int_x^y dz_\nu\rho^{0\nu}(z)\right]. \quad (12)$$

From the above equation, one can see the quark current that couples to the external vector field is expressed in hadronic d.o.f. With this matching, we can calculate the quark distribution function in a proton using the convolution form. The splitting function or the pion distribution in the convolution form is obtained from the pion operator $\mathcal{O}^{\pi^+}_{\rm tot}$. It can be separated into two terms as

$$\mathcal{O}^{\pi^+}_{\rm tot} = \mathcal{O}^{\pi^+} + \mathcal{O}^{\pi^+}_{\rm Sivers}, \tag{13}$$

where

$$\mathcal{O}^{\pi^+}_{\rm Sivers} = [\pi^-(y^-,\vec{y}_\perp)\partial^+\pi^+(0) - \partial^+\pi^-(y^-,\vec{y}_\perp)\pi^+(0)] \times\sqrt{2}g\left\{\int_0^\infty dz^-\rho^{0+}(z^-,0) + \int_\infty^{y^-} dz^-\rho^{0+}(z^-,\vec{y}_\perp)\right\}. \tag{14}$$

The first term in the above equation $\mathcal{O}^{\pi^+}$ is the ordinary bilocal pion operator defined in Eq. (4). For the T-even distributions, this term is dominant and vector meson contribution from the second term can be ignored. However, for the Sivers distribution function, $\mathcal{O}^{\pi^+}$ gives no contribution and $\mathcal{O}^{\pi^+}_{\rm Sivers}$ is crucial to get the nonzero value. With the above operator on the hadronic d.o.f., we can get the Sivers distribution function of a pion in proton $f_{1T}^{\pi/p}(z,\vec{k}_{\perp\pi})$ as

$$\frac{\epsilon^{ji}k^i_{\perp\pi}S^j_\perp}{m_p}f_{1T}^{\pi/p}(z,\vec{k}_{\perp\pi}) = \frac{1}{2}\int\frac{dy^-d^2\vec{y}_\perp}{(2\pi)^3}e^{-i(zP^+y^- - \vec{y}_\perp\cdot\vec{k}_{\perp\pi})}\langle P,\vec{S}_\perp|\mathcal{O}^{\pi}_{\rm Sivers}|P,\vec{S}_\perp\rangle. \tag{15}$$

It can be calculated with the chiral Lagrangian, and the leading loop diagrams are plotted in Fig. 1, where the solid, dashed, double dashed, and double solid lines are for octet baryons, pseudoscalar mesons, vector mesons, and decuplet baryons, respectively. The thick solid line is the eikonal propagator, and the dotted line means the on-shell cut. The effective πNN and $\pi N\Delta$ interaction can be written as $(g_A/\sqrt{2}f_\pi)\bar{N}\partial\!\!\!/\gamma_5\vec{\pi}\cdot\vec{\tau}N$ and $(6g_A/5f_\pi)\bar{N}[g_{\mu\nu}+z\gamma_\mu\gamma_\nu]\partial^\nu\vec{\pi}\cdot\vec{I}\Delta^\mu$ [42]. $g_A = 1.26$ is the axial charge. z is the off-shell parameter, and our results are independent of z because the intermediate decuplet is on-shell. There are several ways of incorporating vector mesons into chiral Lagrangians [43–45]. In this paper, the Lagrangians for the ρNN, $\rho\Delta\Delta$, and $\rho N\Delta$ interactions are obtained from Refs. [46–48] by substituting eQA_μ with gV_μ. They are expressed as

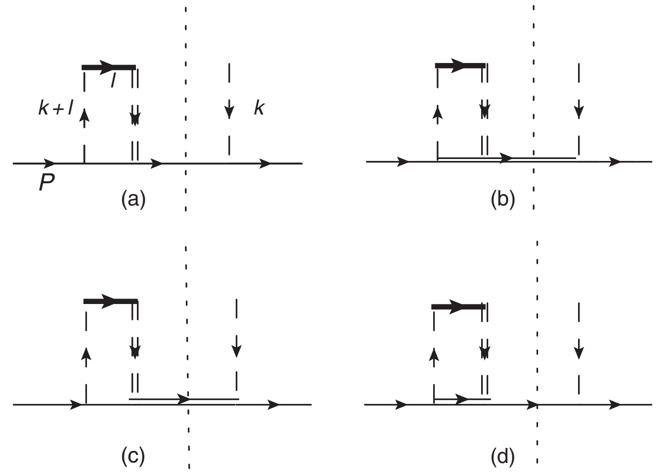

FIG. 1. The Sivers distribution functions of pseudoscalar mesons in the nucleon. The solid, dashed, double dashed, and double solid lines are for the octet baryons, pseudoscalar mesons, vector mesons, and decuplet baryons, respectively. The thick solid line is the eikonal propagator and the dotted line means the on-shell cut.

$$\mathcal{L}_{\rho NN} = -g\bar{N}\left(\gamma^\mu - \kappa_N\frac{\sigma^{\mu\nu}\partial_\nu}{2m_N}\right)\vec{\rho}_\mu\cdot\vec{\tau}N,$$
$$\mathcal{L}_{\rho\Delta\Delta} = -g\bar{\Delta}_\alpha\left(\gamma^{\alpha\beta\mu} + g^{\alpha\beta}\kappa_\Delta\frac{\sigma^{\mu\nu}\partial_\nu}{2m_\Delta}\right)\vec{\rho}_\mu\cdot\vec{\Sigma}\Delta_\beta,$$
$$\mathcal{L}_{\rho N\Delta} = -i\frac{gG^M_{N\Delta}}{2m_N}\bar{N}\gamma^\mu\gamma^5(\partial_\mu\vec{\rho}_\nu - \partial_\nu\vec{\rho}_\mu)\cdot\vec{I}\Delta^\nu + \text{H.c.}, \tag{16}$$

where $1+\kappa_\Delta = \frac{3}{5}(1+\kappa_N)$, $G^M_{N\Delta} = \frac{6\sqrt{2}}{5}(1+\kappa_N)$ according to the quark model [49], and the value of κ_N is 6.1 ± 0.2 [50]. $\vec{\Sigma}$ and $\vec{I}$ are the isospin 3/2 and isospin transition matrices [51]. For the intermediate octet baryons, the contribution to $f_{1T}^{\pi/p}(z,\vec{k}_{\perp\pi})$ is written as

$$\frac{\epsilon^{ji}k^i_{\perp\pi}S^j_\perp}{m_p}f_{1T}^{\pi/p}(z,\vec{k}_{\perp\pi}) = \frac{ig^2g_A^2}{4f_\pi^2}\int\frac{d^4k}{(2\pi)^4}\int\frac{d^4l}{(2\pi)^4}\bar{U}(P,\vec{S}_\perp) \times k\!\!\!/\gamma^5S_{\rm on}(P-k)V_\mu(l)S(P-k-l)\gamma^5(k\!\!\!/+l\!\!\!/)U(P,\vec{S}_\perp) \times\frac{(2k^+ + l^+)}{(l^+ + i\epsilon)}S_\pi(k)S^{\mu+}_\rho(l)S_\pi(k+l) \times\delta(k^+ - zP^+)\delta^2(\vec{k}_\perp - \vec{k}_{\perp\pi}) + \text{H.c.}, \tag{17}$$

where $V_\mu(l)$ is the vertex of the interaction between the nucleon and the ρ meson expressed as $V_\mu(l) = \gamma_\mu + i\kappa_N\frac{\sigma_{\mu\nu}l^\nu}{2m_N}$. S, S_π, and $S^{\mu+}_\rho$ are the propagators of the nucleon, π and ρ, respectively. $S_{\rm on}$ is the on-shell nucleon propagator expressed as $S_{\rm on}(k) = 2\pi(k\!\!\!/+m_N)\delta(k^2-m_N^2)$. The imaginary part of the eikonal propagator $1/(l^+ + i\epsilon)$

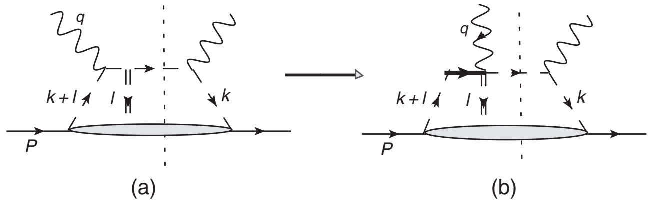

FIG. 2. Final-state interaction in the Sullivan process with collinear approximation. The dashed, double dashed, and waved lines are for the pseudoscalar mesons, vector mesons, and photons respectively. The gray bubble represents octet and decuplet baryons.

gives the real Sivers distribution function of a pion in the nucleon. The expressions for the other diagrams with decuplet intermediate states are similar but more complicated.

The nonzero Sivers distribution function can also be explained from the final-state interaction (FSI). Our approach can be applied in a nonperturbative QCD regime, where the final-state interaction is described by the pion-baryon interaction. The left diagram in Fig. 2 denotes the FSI in Sullivan process, where the momenta k and l are collinear with the proton momentum P in collinear approximation. The "+" component of the momentum is much larger than the other components. As a result, the vector meson projects into the "+" direction at leading order. In other words, the leading part of the momentum of the pseudoscalar meson after the photon scattering is the "−" component. This is also consistent with the analysis of parton distributions in Ref. [20]. Therefore, the $\rho\pi\pi$ vertex and pseudoscalar propagator turn into the eikonal propagator approximately as

$$\frac{(2k+2q+l)^-}{(k+q+l)^2-M^2} \approx \frac{(2k+2q+l)^-}{(2k+2q+l)l+i\epsilon} \approx \frac{1}{l^+ + i\epsilon}. \qquad (18)$$

Accordingly, the diagram Fig. 2(a) can be changed into Fig. 2(b), which means the final-state interaction effect has been absorbed into the distribution functions of a pion in the nucleon. As a result the Sivers distribution function of a pion in the nucleon can be extracted, and it is consistent with the gauge link approach in Fig. 1. In the calculation with spectator model based on the quark-gluon interaction, a similar diagram as Fig. 2(b) is plotted to show that the effect of the final-state interaction can be absorbed into the distribution functions of the target nucleon [10].

With the above splitting function, the Sivers distribution function of sea quark $\bar{q}$ in proton can be obtained by the convolution form, where the sea quark distributions can be expressed in terms of the splitting function and quark distribution in a pion [25,26]. For the TMD distributions, the convolution form is similar. For example, the antidown quark Sivers function in proton can be expressed as

$$\begin{aligned}\frac{\epsilon^{ji} k_\perp^i S_\perp^j}{m_p} f_{1T}^{\bar{d}/p}(x, \vec{k}_\perp) = {}& \frac{i g^2 g_A^2}{4 f_\pi^2} \int_0^1 \frac{dz}{z} \theta(z-x) \int \frac{d^4 l d^4 k_\pi}{(2\pi)^8} \delta(zP^+ - k_\pi^+) \bar{U}(P, \vec{S}_\perp) \not{k}_\pi \gamma^5 S_{\rm on}(P-k_\pi) V_\mu(l) \\ & \times S(P-k_\pi-l)\gamma^5(\not{k}_\pi + \not{l}) U(P, \vec{S}_\perp) \frac{2k_\pi^+}{(l^+ + i\epsilon)} S_\pi(k_\pi) S_\rho^{\mu +}(l) S_\pi(k_\pi + l) \\ & \times \frac{-1}{2} \int \frac{d^4 l_1}{(2\pi)^3} {\rm Tr}[\gamma^+(-\not{l}_1 + m_q)\Gamma(k_\pi, l_1)(\not{k}_\pi - \not{l}_1 + m_q)\Gamma(k_\pi, l_1)(-\not{l}_1 + m_q)] \\ & \times \delta((k_\pi - l_1)^2 - m_q^2)\delta\left(l_1^+ - \frac{x}{z} k_\pi^+\right)\delta^2\left(\vec{l}_{1\perp} - \vec{k}_{1\perp} - \frac{x}{z}\vec{k}_{\perp\pi}\right), \end{aligned} \qquad (19)$$

where $\Gamma(k_\pi, l_1)$ is the quark-meson coupling vertex. The first two rows on the right hand side of the above equation correspond to the π Sivers function written in Eq. (17), while the last two rows are for the antidown quark distribution in π defined as

$$f_{1v}^{\bar{d}/\pi}(y, \vec{k}_{1\perp}) = -\frac{1}{2} \int \frac{d\xi^- d^2 \vec{\xi}_\perp}{(2\pi)^3} e^{iyk_\pi^+ \xi^- - i(\vec{k}_{1\perp} + y\vec{k}_{\pi\perp}) \cdot \vec{\xi}_\perp} \langle \pi^+ | \mathcal{O}^d | \pi^+ \rangle, \qquad (20)$$

where $\mathcal{O}^d = \bar{d}(\xi^-, \vec{\xi}_\perp)\gamma^+ d(0)$. Therefore, Eq. (19) can be expressed by the convolution form as

$$k_\perp^i f_{1T}^{\bar{q}/p}(x, \vec{k}_\perp) = \int d^2 \vec{k}_{\perp\pi} k_{\perp\pi}^i \int_x^1 \frac{dz}{z} f_{1v}^{\bar{q}/\pi}\left(\frac{x}{z}, \vec{k}_\perp - \frac{x}{z}\vec{k}_{\perp\pi}\right) f_{1T}^{\pi/p}(z, \vec{k}_{\perp\pi}), \qquad (21)$$

where $f_{1v}^{\bar{q}/\pi}(\frac{x}{z}, \vec{k}_\perp - \frac{x}{z}\vec{k}_{\perp\pi})$ is the quark TMD distribution in a pion with the intrinsic transverse momentum $\vec{k}_\perp - \frac{x}{z}\vec{k}_{\perp\pi}$. The first moment of the Sivers distribution function is defined as [30]

$$\Delta^N f_{\bar{q}}^{(1)}(x) = \int d^2 \vec{k}_\perp \frac{-k_\perp^2}{2m_p^2} f_{1T}^{\bar{q}/p}(x, \vec{k}_\perp) = \frac{1}{2m_p^2} \int_1^x d\left(\frac{x}{z}\right) f_{1v}^{\bar{q}/\pi}\left(\frac{x}{z}\right) \int d^2 \vec{k}_{\perp\pi} \vec{k}_{\perp\pi}^2 f_{1T}^{\pi/p}(z, \vec{k}_{\perp\pi}), \qquad (22)$$

where $f_{1v}^{\bar{q}/\pi}(x)$ is the quark distribution in π and it can be obtained from the recent fit at $Q = 0.63$ GeV [52].

III. NUMERICAL RESULTS

In the numerical calculation, the dipole regulator $\tilde{F}_j(k)$ $(j = \pi, \rho)$ is applied to deal with the ultraviolet divergence [24,53]:

$$\tilde{F}_j(k) = \left(\frac{M_j^2 - \Lambda_j^2}{k^2 - \Lambda_j^2}\right)^2. \quad (23)$$

For the pion case, in Ref. [54], the monopole regulator is chosen and the corresponding Λ_π is 0.52 GeV. Here because we include the decuplet intermediate state, the monopole regulator is not sufficient to get rid of the UV divergence in Fig. 1(b). From the previous calculation of electromagnetic form factors, strange form factors, and asymmetry of sea quark distributions of protons, reasonable Λ_π in the dipole regulator is around 1 GeV [55,56]. For the ρ meson, the parameter Λ_ρ was chosen to be 1.85 GeV in Ref. [53]. Therefore, we present the results for the range 0.8 GeV $\le \Lambda_\pi \le$ 1.2 GeV and 1.6 GeV $\le \Lambda_\rho \le$ 2.0 GeV. We should mention that with the regulator, there is no power counting included in our method.

The first moment of the Sivers distribution functions of $\bar{d}$ and $\bar{u}$ is plotted in Fig. 3. The green and yellow bands are for $x\Delta^N f_{\bar{d}}^{(1)}(x)$ and $x\Delta^N f_{\bar{u}}^{(1)}(x)$, respectively. For $\bar{d}$ in proton, the first moment is positive. The maximum value of $x\Delta^N f_{\bar{d}}^{(1)}(x)$ is 0.0008–0.0035 at x around 0.2. It then decreases with increasing x, and when x is larger than 0.6, $x\Delta^N f_{\bar{d}}^{(1)}(x)$ will tend to be zero. For $\bar{u}$ in proton, $x\Delta^N f_{\bar{u}}^{(1)}(x)$ is always negative. The maximum absolute value is about 0.0007–0.0037 at x around 0.15. Similar as for $x\Delta^N f_{\bar{d}}^{(1)}(x)$, when x is larger than 0.6, $x\Delta^N f_{\bar{u}}^{(1)}(x)$ will also approach zero. As many phenomenological extractions, the value of the sea quark Sivers function is very small [29,31].

Our result is consistent with the prediction in the large N_C limit where the absolute values of the Sivers distribution functions of $\bar{d}$ and $\bar{u}$ are the same while their signs are opposite [57]. In Ref. [29], where the data are extracted at $Q = 1$ GeV, the central value of $x\Delta^N f_{\bar{d}}^{(1)}(x)$ is negative, while $x\Delta^N f_{\bar{u}}^{(1)}(x)$ is positive. Considering the sign difference in the definition of the first moment between our Eq. (22) and Eq. (4) in Ref. [29], the two results are consistent with each other. Compared with the results in Ref. [30], where the central values of extracted $x\Delta^N f_{\bar{u}}^{(1)}(x)$ and $x\Delta^N f_{\bar{d}}^{(1)}(x)$ are both negative and the absolute value of $x\Delta^N f_{\bar{d}}^{(1)}(x)$ is much larger than $x\Delta^N f_{\bar{u}}^{(1)}(x)$, our $x\Delta^N f_{\bar{d}}^{(1)}(x)$ has similar magnitudes but with the opposite sign. For $x\Delta^N f_{\bar{u}}^{(1)}(x)$, the sign is the same as their best fit but our magnitude is larger. Hopefully, these differences can be checked by further theoretical and experimental analysis.

For $x\Delta^N f_{\bar{u}}^{(1)}(x)$, only one diagram in Fig. 1(b) gives contribution. However, for $x\Delta^N f_{\bar{d}}^{(1)}(x)$, all the four diagrams in Fig. 1 give contribution. To see the separate contribution clearly, we plot the contribution to $x\Delta^N f_{\bar{d}}^{(1)}(x)$ from different intermediate states in Fig. 4. The dashed, dotted, and dot-dashed lines are for the contributions from the intermediate octet, decuplet, and octet-decuplet transition, respectively. The solid line is the total result. From the figure, we can see that for $x\Delta^N f_{\bar{d}}^{(1)}(x)$, the contributions from the intermediate octet and octet-decuplet transition are dominant. The contribution of the octet-decuplet transition gives a large positive value to $x\Delta^N f_{\bar{d}}^{(1)}(x)$. For the contribution from the octet intermediate state, the sign is x dependent. It is negative at small x and when $x > 0.1$, the sign changes to

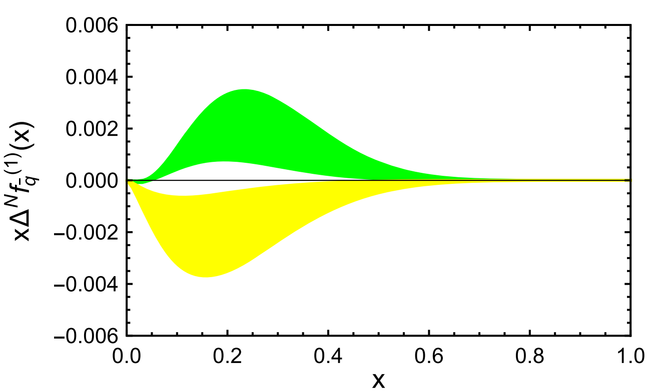

FIG. 3. The first momentum of sea quark Sivers distribution functions versus x at $Q = 0.63$ GeV. The green and yellow bands are the results of $x\Delta^N f_{\bar{d}}^{(1)}(x)$ and $x\Delta^N f_{\bar{u}}^{(1)}(x)$ with 0.8 GeV $\le$ $\Lambda_\pi \le$ 1.2 GeV and 1.6 GeV $\le \Lambda_\rho \le$ 2.0 GeV.

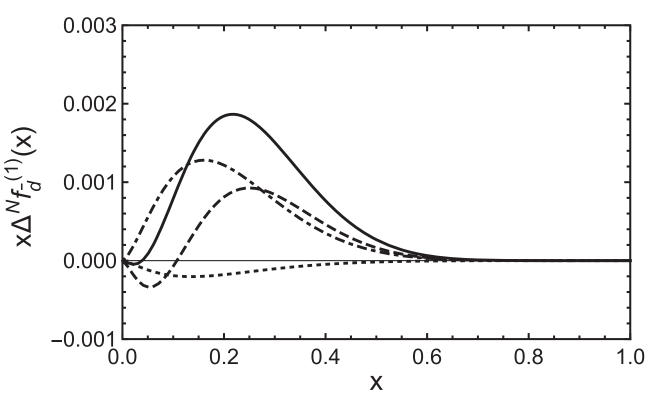

FIG. 4. Contributions to $x\Delta^N f_{\bar{d}}^{(1)}(x)$ from different intermediate states with $\Lambda_\pi = 1$ GeV, $\Lambda_\rho = 1.85$ GeV, and $\kappa_N = 6.1$. The dashed, dotted, and dot-dashed lines are for the contributions from the intermediate octet, decuplet, and octet-decuplet transition, respectively. The solid line is for the total result.

be positive. The contribution to $x\Delta^N f_{\bar{d}}^{(1)}(x)$ from the decuplet intermediate state is very small. The decuplet intermediate state gives negative contribution to both $x\Delta^N f_{\bar{d}}^{(1)}(x)$ and $x\Delta^N f_{\bar{u}}^{(1)}(x)$. However, the contribution to $x\Delta^N f_{\bar{d}}^{(1)}(x)$ is 9 times smaller than that to $x\Delta^N f_{\bar{u}}^{(1)}(x)$ due to the smaller value of the coupling constants for the π^+ case than for the π^- case.

Our calculation with the chiral Lagrangian is valid at the low energy scale. The result is supposed to hold up to the scale of ρ meson mass or 1 GeV ($4\pi f_\pi$). This is why the input scale of the pion PDF is chosen to be at 0.63 GeV. The scale evolution of the Sivers function as well as the first momentum $\Delta^N f_{\bar{q}}^{(1)}(x)$ is discussed in [58–60]. With the scale increasing, the maximum of $x\Delta^N f_{\bar{d}}^{(1)}(x)$ and $x\Delta^N f_{\bar{u}}^{(1)}(x)$ will become smaller due to the effect of diagonal terms in the twist-3 evolution kernel [32].

IV. SUMMARY

In summary, we proposed a mechanism for the study of the Sivers distribution function with the chiral Lagrangian. The vector meson is introduced for the $SU(2)_V$ hidden symmetry. The bilocal π operator is redefined with the gauge link of the vector meson which is locally $SU(2)$ invariant. The eikonal propagator generated from the flavor gauge link is crucial to obtaining a nonzero Sivers distribution function. The gauge link approach is also proven to be consistent with the final-state interaction in the collinear approximation. With the convolution form, which combines the splitting function calculated from the bilocal π operator and the valence quark distribution in pion, the Sivers distribution functions of $\bar{u}$ and $\bar{d}$ are obtained. Numerical results show that the absolute values of $x\Delta^N f_{\bar{u}}^{(1)}(x)$ and $x\Delta^N f_{\bar{d}}^{(1)}(x)$ are close to each other, while their signs are opposite. For $x\Delta^N f_{\bar{d}}^{(1)}(x)$, the contributions from the intermediate octet state and octet-decuplet transition are dominant. The decuplet intermediate state gives negligible contribution. For $x\Delta^N f_{\bar{u}}^{(1)}(x)$ the only contribution comes from the decuplet intermediated state and it is 9 times larger than the corresponding contribution for $x\Delta^N f_{\bar{d}}^{(1)}(x)$. Without any fine tuning of the parameters, our results are consistent with the prediction obtained in the large NC limit, and are also comparable with the recent phenomenological extractions from fitting the experimental data. This is the first theoretical estimation on $x\Delta^N f_{\bar{u}}^{(1)}(x)$ and $x\Delta^N f_{\bar{d}}^{(1)}(x)$ within the framework of the chiral Lagrangian. Our predictions can be checked by the future theoretical and experimental analysis.

ACKNOWLEDGMENTS

This work is supported by the National Natural Sciences Foundations of China under the Grant No. 11475186, the Sino-German CRC 110 “Symmetries and the Emergence of Structure in QCD” project by NSFC under the Grant No. 11621131001, and the Key Research Program of Frontier Sciences, CAS under Grant No. Y7292610K1.

[1] S. Pisano, EPJ Web Conf. **85**, 02033 (2015).
[2] D. Boer and P. J. Mulders, Phys. Rev. D **57**, 5780 (1998).
[3] A. Airapetian *et al.* (HERMES Collaboration), Phys. Rev. Lett. **103**, 152002 (2009).
[4] F. Bradamante (COMPASS Collaboration), J. Phys. Conf. Ser. **938**, 012004 (2017).
[5] D. W. Sivers, Phys. Rev. D **41**, 83 (1990).
[6] A. Bravar (Spin Muon Collaboration), Nucl. Phys. B, Proc. Suppl. **79**, 520 (1999).
[7] A. Airapetian *et al.* (HERMES Collaboration), Phys. Rev. D **64**, 097101 (2001).
[8] X. Ji, Phys. Rev. Lett. **110**, 262002 (2013).
[9] S. J. Brodsky, D. S. Hwang, and I. Schmidt, Phys. Lett. B **530**, 99 (2002).
[10] D. Boer, S. J. Brodsky, and D. S. Hwang, Phys. Rev. D **67**, 054003 (2003).
[11] A. Bacchetta, A. Schaefer, and J.-J. Yang, Phys. Lett. B **578**, 109 (2004).
[12] Z. Lu and B.-Q. Ma, Nucl. Phys. **A741**, 200 (2004).
[13] K. Goeke, S. Meissner, A. Metz, and M. Schlegel, Phys. Lett. B **637**, 241 (2006).
[14] Z. Lu and I. Schmidt Phys. Rev. D **75**, 073008 (2007).
[15] A. Bacchetta, F. Conti, and M. Radici, Phys. Rev. D **78**, 074010 (2008).
[16] T. Maji, D. Chakrabarti, and A. Mukherjee, Phys. Rev. D **97**, 014016 (2018).
[17] F. Yuan Phys. Lett. B **575**, 45 (2003).
[18] A. Courtoy, S. Scopetta, and V. Vento, AIP Conf. Proc. **1105**, 193 (2009).
[19] B. Pasquini and F. Yuan, Phys. Rev. D **81**, 114013 (2010).
[20] A. V. Belitsky, X. Ji, and F. Yuan, Nucl. Phys. **B656**, 165 (2003).
[21] J. C. Collins Phys. Lett. B **536**, 43 (2002).
[22] J. D. Sullivan, Phys. Rev. D **5**, 1732 (1972).
[23] M. Burkardt, K. S. Hendricks, C.-R. Ji, W. Melnitchouk, and A. W. Thomas, Phys. Rev. D **87**, 056009 (2013).

[24] Y. Salamu, C.-R. Ji, W. Melnitchouk, A. W. Thomas, and P. Wang, Phys. Rev. D **99**, 014041 (2019).
[25] Y. Salamu, C.-R. Ji, W. Melnitchouk, and P. Wang, Phys. Rev. Lett. **114**, 122001 (2015).
[26] X. G. Wang, C.-R. Ji, W. Melnitchouk, Y. Salamu, A. W. Thomas, and P. Wang, Phys. Lett. B **762**, 52 (2016).
[27] L. Adamczyk *et al.* (STAR Collaboration), Phys. Rev. Lett. **116**, 132301 (2016).
[28] J. Huang, Z.-B. Kang, I. Vitev, and H. Xing, Phys. Rev. D **93**, 014036 (2016).
[29] A. Bacchetta and M. Radici, Phys. Rev. Lett. **107**, 212001 (2011).
[30] M. Anselmino, M. Boglione, U. D'Alesio, F. Murgia, and A. Prokudin, J. High Energy Phys. 04 (2017) 046.
[31] A. Martin, F. Bradamante, and V. Barone, Phys. Rev. D **95**, 094024 (2017).
[32] M. Boglione, U. D'Alesio, C. Flore, and J. O. Gonzalez-Hernandez, J. High Energy Phys. 07 (2018) 148.
[33] A. Bacchetta, U. D'Alesio, M. Diehl, and C. A. Miller, Phys. Rev. D **70**, 117504 (2004).
[34] X.-d. Ji and F. Yuan, Phys. Lett. B **543**, 66 (2002).
[35] J.-W. Chen and X.-d. Ji, Phys. Rev. Lett. **87**, 152002 (2001); **88**, 249901(E) (2002).
[36] M. Bando, T. Kugo, S. Uehara, K. Yamawaki, and T. Yanagida, Phys. Rev. Lett. **54**, 1215 (1985).
[37] M. Bando, T. Kugo, and K. Yamawaki, Phys. Rep. **164**, 217 (1988).
[38] M. Tanabashi, Phys. Lett. B **384**, 218 (1996).
[39] K. Kawarabayashi and M. Suzuki, Phys. Rev. Lett. **16**, 255 (1966).
[40] Riazuddin and Fayyazuddin, Phys. Rev. **147**, 1071 (1966).
[41] M. Tanabashi *et al.* (Particle Data Group), Phys. Rev. D **98**, 030001 (2018).
[42] S. Scherer, Adv. Nucl. Phys. **27**, 277 (2003).
[43] J. Schechter, Phys. Rev. D **34**, 868 (1986).
[44] K. Yamawaki, Phys. Rev. D **35**, 412 (1987).
[45] U. G. Meissner and I. Zahed, Z. Phys. A **327**, 5 (1987).
[46] E. E. Jenkins, Nucl. Phys. **B368**, 190 (1992).
[47] L. S. Geng, J. M. Camalich, and M. J. V. Vacas, Phys. Rev. D **80**, 034027 (2009).
[48] H. F. Jones and M. D. Scadron, Ann. Phys. (N.Y.) **81**, 1 (1973).
[49] G. E. Brown and W. Weise, Phys. Rep. **22**, 279 (1975).
[50] P. Mergell, U. G. Meissner, and D. Drechsel, Nucl. Phys. **A596**, 367 (1996).
[51] J. Haidenbauer, S. Petschauer, N. Kaiser, U.-G. Meißner, and W. Weise, Eur. Phys. J. C **77**, 760 (2017).
[52] M. Aicher, A. Schafer, and W. Vogelsang, Phys. Rev. Lett. **105**, 252003 (2010).
[53] R. Machleidt, Adv. Nucl. Phys. **19**, 189 (1989).
[54] P. C. Barry, N. Sato, W. Melnitchouk, and C.-R. Ji, Phys. Rev. Lett. **121**, 152001 (2018).
[55] F. He and P. Wang Phys. Rev. D **98**, 036007 (2018).
[56] Y. Salamu, C.-R. Ji, W. Melnitchouk, A. W. Thomas, P. Wang, and X. G. Wang, arXiv:1907.08551.
[57] P. V. Pobylitsa, arXiv:hep-ph/0301236.
[58] S. M. Aybat, J. C. Collins, J.-W. Qiu, and T. C. Rogers, Phys. Rev. D **85**, 034043 (2012).
[59] M. Anselmino, M. Boglione, and S. Melis, Phys. Rev. D **86**, 014028 (2012).
[60] Z.-B. Kang and J.-W. Qiu, Phys. Lett. B **713**, 273 (2012).